AD-A128 675 FLOW PROBLEMS IN TURBOMACHINES(U) MICHIGAN UNIV ANN ARBOR DEPT OF AEROSPACE ENGINEERING T C ADAMSON ET AL. 15 APR 83 N00014-79-C-0285 1/1

UNCLASSIFIED F/G 20/4 NL

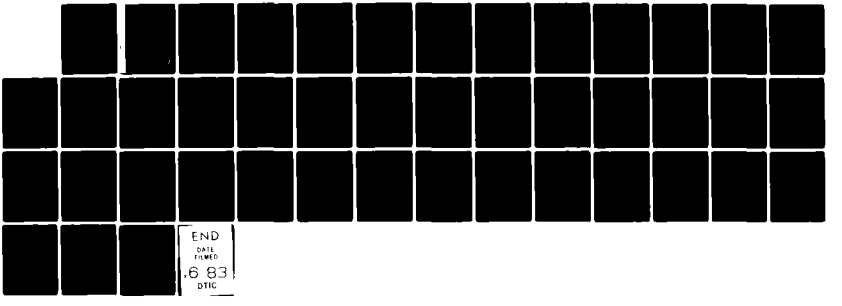

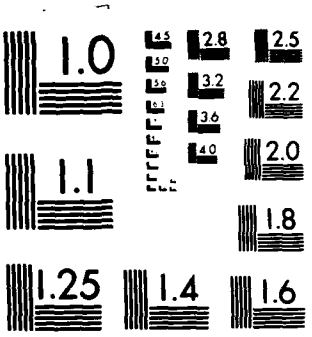

(12)

Annual Report No. 1
Contract N00014-79-C-0285; NR 094-395

FLOW PROBLEMS IN TURBOMACHINES

Thomas C. Adamson Jr.
and
Arthur F. Messiter

Department of Aerospace Engineering
The University of Michigan
Ann Arbor, MI 48109

15 April 1983

Annual Report For Period
1 March 1982 - 28 February 1983

Approved for public release; distribution unlimited.

Prepared for :
Office Of Naval Research
800 N. Quincy Street
Arlington Va 22217

SECURITY CLASSIFICATION OF THIS PAGE (When Data Entered)

REPORT DOCUMENTATION PAGE	READ INSTRUCTIONS BEFORE COMPLETING FORM
1. REPORT NUMBER: ANNUAL REPORT NO. 1	2. GOVT ACCESSION NO.: AD-A128675
3. RECIPIENT'S CATALOG NUMBER	
4. TITLE (and Subtitle): FLOW PROBLEMS IN TURBOMACHINERY	5. TYPE OF REPORT & PERIOD COVERED: ANNUAL, 1 Mar 1982 - 28 Feb 1983
	6. PERFORMING ORG. REPORT NUMBER
7. AUTHOR(s): THOMAS C. ADAMSON, JR. ARTHUR F. MESSITER	8. CONTRACT OR GRANT NUMBER(s): N00014-79-C-0285
9. PERFORMING ORGANIZATION NAME AND ADDRESS: DEPARTMENT OF AEROSPACE ENGINEERING THE UNIVERSITY OF MICHIGAN ANN ARBOR, MICHIGAN 48109	10. PROGRAM ELEMENT, PROJECT, TASK AREA & WORK UNIT NUMBERS: 61153N RR024-03-01 094-395
11. CONTROLLING OFFICE NAME AND ADDRESS: OFFICE OF NAVAL RESEARCH 800 NORTH QUINCY STREET ARLINGTON, VIRGINIA 22217	12. REPORT DATE: 15 April 1983
	13. NUMBER OF PAGES: 36
14. MONITORING AGENCY NAME & ADDRESS (if different from Controlling Office)	15. SECURITY CLASS. (of this report): Unclassified
	15a. DECLASSIFICATION/DOWNGRADING SCHEDULE

16. DISTRIBUTION STATEMENT (of this Report)

Approved for Public Release; Distribution Unlimited

17. DISTRIBUTION STATEMENT (of the abstract entered in Block 20, if different from Report)

18. SUPPLEMENTARY NOTES

19. KEY WORDS (Continue on reverse side if necessary and identify by block number)

CASCADES
TRANSONIC FLOW
SUPERSONIC FLOW
TURBULENT BOUNDARY LAYER

20. ABSTRACT (Continue on reverse side if necessary and identify by block number)

A brief discussion is given of the work done on the three problems studied during the period covered by this report. The problems considered are: (1) transonic flow through heavily loaded cascades, (2) transonic flow through a three-dimensional compressor rotor, and (3) supersonic flow with a turbulent boundary layer at a ramp.

DD FORM 1 JAN 73 1473

SECURITY CLASSIFICATION OF THIS PAGE (When Data Entered)

FLOW PROBLEMS IN TURBOMACHINERY

by

THOMAS C. ADAMSON, JR.
ARTHUR F. MESSITER

Department of Aerospace Engineering
The University of Michigan

Technical Report

prepared for

Office of Naval Research
800 North Quincy Street
Arlington, Virginia 22217

Contract No. N00014-79-C-0285
Work Unit No. 094-395

April 1983

Introduction

The desire to obtain ever greater performance from jet engines with smaller and smaller diameters has forced the engine designer to consider relatively complex flow problems. Thus, in most modern jet engines, the flow relative to the compressor or fan rotor blades in the first few stages is in the transonic regime. At the tip, supersonic velocities occur and it may soon be the case that supersonic relative velocities are found over a large portion of the blades.

Because flows in the transonic and supersonic regimes are so much more complex, in general, than those found when compressibility effects are negligible, the computational problems which must be solved in order to predict the flow fields over arbitrary geometries are much more difficult. Both analytical and numerical efforts are required.

The present contract is concerned with problems, associated with engines, involving both transonic and supersonic flow fields. Generally, asymptotic methods have been used in the analyses, with numerical computations being used sometimes only to evaluate analytical results and at other times to find the complete solution in a region for which analytical solutions are not available. In this way, it is hoped to find relatively efficient means of solution which will both exhibit the understanding given by analytical solutions and utilize the computational power offered by the computer in handling problems insoluble by other means.

Summary of Results; Implications of Work

The research carried out during the past contract year (March 1, 1982 to February 28, 1983) was concerned with three problems: (1) transonic

flow through heavily loaded cascades, (2) transonic flow through three-dimensional compressor rotors, and (3) the supersonic turbulent boundary layer at a ramp.

The first problem is an extension of previous work done on transonic flow over a lightly loaded cascade.[1] The methods and ideas used in obtaining the latter solutions are being used in analysing the heavily loaded case, which corresponds to conditions considered in present-day and future jet engines. In particular, attention is being focused on the formation of supercritical regions, with and without shock waves, on the suction surfaces of the blades. This is a very important part of the flow field since shock waves cause losses and perhaps separation. At the present time, the governing equations valid in each region have been derived to the desired order of approximations and solutions have been found in one region. The work is the subject of a Ph.D. dissertation.

The second problem, *transonic flow through a three-dimensional compressor rotor*, has been in progress for some time. It is an extension of the work done on lightly loaded cascades to three dimensions, and thus is very complex. Since the solutions are, with the exception of those in one region, analytical, they should prove very beneficial in explaining the detailed flow picture in a rotor. Considerable time has been spent in finding the numerical solutions in the one region in which this is necessary and in joining this and the analytical results in composite solutions which can be used for the calculation of numerical examples. This work is finally nearing completion. A paper will be written and submitted for publication.

The third problem, supersonic turbulent boundary layer at a ramp, has been completed and a Ph.D. dissertation has been written. The solutions

obtained allow one to calculate the pressure and wall shear stress distributions for unseparated flow downstream of the leading edge of the ramp, for a relatively large range of supersonic Mach numbers and ramp angles. The results are entirely analytical so that no complex numerical schemes are needed. The surface pressure distribution is in close agreement with experiment for cases in which the flow appears to be unseparated. The calculated wall shear stress is within about 10% of the experimental data in the case compared, even though a simple mixing-length eddy-viscosity model is employed. A journal article covering this work is being written.

A detailed description of the work done on the above problems is contained in a following section.

Publications and Invited Talks

The following publications are based on work supported by this contract.

(1) Adamson, T. C. and Sichel, M. (1982), "Transonic Shear Flow in a Three-Dimensional Channel." J. Fluid Mech., vol. 123, pp. 443-457.

(2) Agrawal, S. "Asymptotic Theory of an Unseparated Supersonic Turbulent Boundary Layer at a Compression Corner." Ph.D. Thesis, Univ. of Michigan, 1983 (Chairman of Dissertation Committee, A. F. Messiter).

In addition, Prof. T. C. Adamson has been invited to give a talk on the analysis of supersonic inlet diffusers at the ONR/AFOSR Workshop on Mechanisms of Instability in Liquid Fueled Ramjets, and to give a seminar at SUNY at Buffalo on Asymptotic Methods in Internal Transonic Flows; both of these talks are to be given in March, 1983. Both are concerned with work supported by ONR either through Project SQUID or the present contract. Also, Prof. A. F. Messiter has written an invited review article

on boundary-layer interaction theory, one section of which discusses the theoretical background for the work done on the ramp problem studied under this contract.

Discussion of Work

(1) Transonic Flow through Heavily Loaded Cascades

The first cascade problem studied under ONR (Project SQUID) support was that of a lightly loaded cascade in transonic flow.[1] The term "lightly loaded" refers to the fact that the blade thickness, maximum camber, and angle of attack were all of the same order, and in a certain sense small compared to the order of corresponding terms in typical single airfoil theory. If M_o is the Mach number in the incoming flow far upstream of the cascade, these three parameters were all $O((M_o^2-1)^2)$ whereas according to the transonic similarity law for single airfoils they would be $O((M_o^2-1)^{3/2}$; since the flow is transonic, $M_o^2-1 \ll 1$. The result of this ordering is that the lift forces on the blades are thus relatively smaller than in the single airfoil case; the blades are said to be lightly loaded. This set of conditions was chosen for study because the resulting flow problem is easier to solve and yet has technical relevance; moreover, it gives important information concerning the structure of the flow field. It is a good first problem, and the experience gained from it has been used to formulate the more demanding problem of a heavily loaded cascade.

A sketch indicating the geometry considered and the notation used is shown in Figure 1. An inviscid, steady, transonic flow of a perfect gas with constant specific heats is considered. A small parameter ε is introduced such that $\varepsilon = O(M_o^2-1)$, as in the previous work. The blades in the cascade have shapes given by

$$y_u = y_o + \varepsilon^{3/2} f_u(x) + \varepsilon^2 g_u(x) - x\alpha \qquad (1a)$$

$$y_\ell = y_o - \varepsilon^{3/2} f_\ell(x) - \varepsilon^2 g_\ell(x) - x\alpha \qquad (1b)$$

where y_0 is the position of the leading edge of the blade in question, α is the angle of attack ($\alpha=O(\varepsilon^{3/2})$), and the subscripts u and ℓ refer to upper and lower surfaces of the blade respectively. All lengths are made dimensionless with respect to the blade chord. Thus the thickness-to-chord ratio is $O(\varepsilon^{3/2})$ for this case; a convenient definition of ε is obtained by setting $\varepsilon^{3/2}$ equal to the thickness ratio. The incoming flow velocity is written as

$$u_0 = 1 \pm K_1\varepsilon \pm K_{3/2}\varepsilon^{3/2} + \ldots \tag{2}$$

where the K_i are constants, + and - refer to supersonic and subsonic flows respectively, and all velocities are dimensionless with respect to the sonic velocity in the incoming flow. Because the flow is transonic, shock waves are weak enough that to the order retained a velocity potential may be considered. A perturbation potential ϕ is defined by

$$u = u_0 + \phi_x \qquad v = \phi_y \tag{3a,b}$$

The governing equations are the gasdynamic and energy equations:

$$a^2\nabla\cdot\vec{q} = (\vec{q}\cdot\nabla)\frac{q^2}{2} \tag{4a}$$

$$\frac{a^2}{\gamma-1} + \frac{q^2}{2} = \frac{1}{\gamma-1} + \frac{u_0^2}{2} \tag{4b}$$

where the vector velocity $\vec{q}$ has components u and v, and where γ is the ratio of specific heats. If Eqns. (3a,b) and (4b) are substituted into (4a), a single equation for ϕ results. The boundary conditions are given by

$$(v/u)_{u,\ell} = dy_{u,\ell}/dx \tag{5}$$

As in the lightly loaded cascade analysis, the flow field can be divided into several regions, illustrated in Fig. 2 . In the region marked "c", there is a channel flow bounded by the two blades. Because the channel walls are not symmetric and because the slopes of the walls are $O(\varepsilon^{3/2})$, the same as the thickness ratio, the expansion for ϕ in the channel can be shown to be as follows:

$$\phi = \varepsilon^{3/4}\phi_1 + \varepsilon\phi_2 + \varepsilon^{5/4}\phi_3 + \varepsilon^{3/2}\phi_4 + \ldots \qquad (6)$$

That is, the expansion proceeds in powers of $\varepsilon^{1/4}$ rather than in powers of $\varepsilon^{1/2}$ as in the lightly loaded case. Although this expansion is more complicated in that more terms are required, the first dependence upon y occurs in ϕ_4; ϕ_1,ϕ_2, and ϕ_3 are all dependent upon x alone because the boundary conditions give $\frac{\partial \phi_i}{\partial y} = 0$ until those for ϕ_4 are reached. Solutions for this region, valid to order ε^2, have been found, i.e. solutions for ϕ_1, ϕ_2, ϕ_3, and ϕ_4 are known.

Upstream of the channel, in the region marked "U" in Fig. 2 , the expansion shown in Eq. 6 and the same governing equations found in the channel flow analysis hold for each ϕ_i for $y = O(1)$. The essential difference, of course, is the fact that there is no outer wall or blade; only one boundary condition can be used. Therefore, it is necessary to find an outer solution, for the region "O" in Fig. 2, in which $y\varepsilon^{1/2} = O(1)$; that is, since $\varepsilon << 1$, $y >> 1$ in this region. If $y = \lambda x$ along the line passing through each of the leading edges of the cascade (Fig. 1), then the independent variables, the expansion for ϕ, and the governing equation for the lowest order term in ϕ are, respectively,

$$\tilde{y} = (\varepsilon k_1)^{1/2}(y-\lambda x) \qquad \tilde{x} = x \tag{7a,b}$$

$$\phi = \varepsilon\tilde{\phi}_1(\tilde{x},\tilde{y}) + \varepsilon^{3/2}\tilde{\phi}_{3/2}(\tilde{x},\tilde{y}) + \ldots \tag{7c}$$

$$((\gamma+1)\tilde{\phi}_{1\tilde{x}} \pm k_1)\tilde{\phi}_{1\tilde{x}\tilde{x}} - k_1\tilde{\phi}_{1\tilde{y}\tilde{y}} = 0 \tag{7d}$$

where $k_1 = 2K_1$. Thus, the nonlinear transonic small-disturbance equation holds for the far field, as opposed to the Laplace or wave equation which was found in the case of lightly loaded blades. The boundary condition is the same, in principle; that is, in $\tilde{x},\tilde{y}$ coordinates, the cascade appears as a periodic cusped wall as $\tilde{y} \to 0$ with period d, where d is defined as Fig. 1. As $\tilde{y} \to 0$, the flow must be tangent to this wall and for subsonic flow, as $y \to \infty$, velocity perturbations tend to zero.

The solution in the outer region must match term by term with the solution valid in the upstream region in the limits $\tilde{y} \to 0$ and $y \to \infty$. This matching is in lieu of the missing boundary conditions and supplies functions and constants necessary to complete the solutions in the upstream regions. From this matching, it is found, for example, that $\phi_1 = 0$ in the upstream region. That is, there is no term $O(\varepsilon^{3/4})$ outside the channel; the lowest order term in u is $O(\varepsilon)$. Because of this difference between the upstream and channel flow solutions, there is another region which must be considered, the inner region marked "I" in Fig. 2.

In the inner region, where $x - d << 1$, the perturbation in the flow velocity u becomes stronger, going from $O(\varepsilon)$ to $O(\varepsilon^{3/4})$ as the channel is entered. One expects the flow acceleration to be important here so that velocity changes are large enough that the nonlinear equation is needed. One can show that in order for this to be true, the inner region must be $O(\varepsilon^{1/2})$ in thickness. Thus, since the inner region must be found at any

leading edge, the dependent variables, expansion for ϕ, and lowest order governing equation are, respectively,

$$x^* = \frac{\pi(x-nd)}{\varepsilon^{1/2}\ell} \qquad y^* = \frac{\pi(y-n\ell)}{\ell} \qquad n=0, \pm 1, \pm 2,... \tag{8a,b}$$

$$\phi = \frac{\ell}{\pi}\left(\varepsilon^{3/2}\phi_1^*(x^*,y^*) + \varepsilon^{7/4}\phi_2^*(x^*,y^*) + ...\right) \tag{8c}$$

$$((\gamma+1)\phi_{1x^*}^* \pm k_1)\phi_{1x^*x^*}^* - \phi_{1y^*y^*}^* = 0 \tag{8d}$$

where ℓ is the blade spacing. (Fig. 1). Boundary conditions are given by the tangency conditions at the airfoil surfaces, and the solutions must match with the outer and channel flow solutions in the proper limits. The latter matching condition is of interest here because of the aforementioned change of order of $u-u_o$ as the inner region is traversed. From Eqs. (8a) and (8c),

$$\phi_x = \varepsilon\phi_{1x^*}^* + ... \tag{9}$$

so, first, as $x^* \to -\infty$ $\phi_{1x^*}^* \sim \phi_{2x}(d)$, a constant. Now in the channel, it is found that

$$\ell(\gamma+1)\phi_{1x}\phi_{1xx} = -f_u'(x) - f_\ell'(x-d) \tag{10}$$

Hence, as $x \to d$, with $\phi_{1x}(d) = 0$ because there is no term of $O(\varepsilon^{3/4})$ for matching,

$$\phi_{1x}^2 \sim (x-nd) \text{ constant} = \varepsilon^{1/2}x^* \text{ constant}$$

or

$$\varepsilon^{3/4}\phi_{1x} \sim \text{constant } \varepsilon(x^*)^{1/2} + ... \tag{11}$$

Hence, as $x^* \to \infty$, if

$$\phi^*_{1x^*} \sim (x^*)^{1/2} \text{ constant} + \ldots \tag{12}$$

the solutions will match. Equation (12) then is the boundary condition to be used in the solution of Eq. (8d) as $x^* \to \infty$. It is seen from Eqn. (11) that the lowest order perturbation in u does indeed change order as the flow passes through the inner region into the channel region. Finally, it should be noted that an inner region, formulated in essentially the same way, exists at the trailing edge of each airfoil; since no fundamentally new ideas are involved in its description, it will not be considered further here.

When compared to the corresponding development of the problem for the lightly loaded cascade, the above formulation shows some similarities and several differences. In a gross sense, the description of the flow field is the same in each case in that the same regions, with the same scales, are found in each. However, in the heavily loaded case, the solutions in the channel are larger in magnitude at each order of approximation, and the lowest order solutions in the inner and outer regions are governed by nonlinear equations rather than by the linear equations found in the lightly loaded case. This means that numerical computations must be made now to find even the lowest order solutions.

The expansion for u in the region U upstream of the channel can be written as

$$u = a^* + \varepsilon(\phi_{2x} - \frac{2K_1}{\gamma+1}) + \varepsilon^{3/2}(\phi_{4x} - \frac{2K_{3/2}}{(\gamma+1)}) + \ldots \tag{13}$$

because $\phi_{1x} = \phi_{3x} = 0$. That is, $\phi_1(x)$, $\phi_2(x)$, and $\phi_3(x)$ are found by matching with the solutions valid in the outer region and there are no

terms of order $\varepsilon^{3/4}$ or $\varepsilon^{5/4}$ in the expansion for γ in the outer region. In Eq. (13) the incoming flow has been assumed to be subsonic, and

$$a^* = 1 - \left(\frac{\gamma-1}{\gamma+1}\right) \varepsilon K_1 - \left(\frac{\gamma-1}{\gamma+1}\right) \varepsilon^{3/2} K_{3/2} + \ldots .$$

Finally, it is easily shown from Eqn. (4b) that for $u = a = a^*$, $\phi_{2x} = 2K_1/(\gamma+1)$, $\phi_{3/2x} = 2K_{3/2}/(\gamma+1)$, etc.

As the flow accelerates along the upper side of the blade airfoil (in region U) it is possible that a small supersonic region of flow may occur. Thus, supercritical regions of the kind shown in Fig. 3 are found. These regions may or may not be terminated by a shock wave; that is, it is possible to have a "shockless" acceleration and deceleration into and out of the supersonic flow region, and losses in stagnation pressure then do not occur. If the extent of the supercritical region in the y direction is taken to be O(1), then the flow in the outer region is still subsonic and hence to the scale of this outer region the supercritical region is simply a point on the airfoil surface, at which the local velocity can be no higher than sonic velocity. That is, the scale of the supercritical region in the x direction must be small compared to one and it is thus another inner region. Solutions valid in this region must match with the solutions in region U and the outer region. An idea of the scale of this inner region may be gained by consideration of Eqn. (13) in the event that ϕ_{2x} is expanded about a point x_o where the velocity just reaches sonic value; recall that $\phi_{2x} = \tilde{\phi}_{1\tilde{x}}(\tilde{x},0)$ from matching. Then since at x_o ϕ_{2x} is a maximum, a Taylor expansion gives

$$\phi_{2x}(x) = \frac{2K_1}{\gamma+1} + \frac{(x-x_o)^2}{2}\phi_{2xxx}(x_o) + \ldots \qquad (14)$$

Since ϕ_{4x} is a function of both x and y one can write only

$$\phi_{4x}(x,y) = \frac{2K_{3/2}}{(\gamma+1)} + f(x_o,y) + \ldots \qquad (15)$$

when $f(x_o,y) = O(1)$. If Eqns. (14) and (15) are substituted into Eq. (13), it is seen that the term of $O(\varepsilon)$ can decrease as $x \to x_o$ until for $(x-x_o) = O(\varepsilon^{1/4})$, it is $O(\varepsilon^{3/2})$, the order of the next term in the expansion. When two terms become of the same order, then another region may be indicated, in this case $O(\varepsilon^{1/4})$ in length.

When an inner region $\Delta x = O(\varepsilon^{1/4})$ is investigated, it is found that the lowest order governing equation is linear and that the solution describes a shockless supercritical flow region. On the other hand, if it is assumed that the non-linear equation must hold, thus allowing for shock waves, then it is found that the thickness of this inner region must be $O(\varepsilon^{3/4})$. The conditions under which either analysis may hold in the inner region are not yet understood. This is part of the ongoing work which is the subject of a Ph.D. dissertation.

In summary, it has been found that the work done on the lightly loaded cascade[1] has been very beneficial in providing a model of the gross structure of the flow field. The indications are that more numerical work will be required to describe the flow field of a heavily loaded case, as expected. The work is proceeding well and is the subject of a Ph.D. dissertation.

(2) Transonic Flow through a Three-Dimensional Compressor Rotor

This analysis is concerned, again, with lightly loaded blades. However, a three-dimensional rotor is considered rather than just a cascade. The flow is assumed to be inviscid and transonic and is steady in a coordinate system attached to the rotating blades; thus, the results hold for a rotor in the first stage of a compressor or in those cases where the effects of the wakes from blades upstream of the row in question are negligible.

In the coordinate system fixed to the blades, x is the distance along a helical line which has the direction, with respect to the axis, of the incoming flow; this helix can be pictured as being the line traced on a cylinder of constant radius by a fluid particle in the undisturbed flow. The coordinate y gives an angular measure in a direction perpendicular to x at the origin and the z coordinate is in the radial direction. Because the coordinate system is not orthogonal, in general, there are some extra terms introduced into the governing equations. On the other hand, because y measures an angular difference, blades lie along lines y = constant, and, locally, the picture of the flow field on an x,y plane, z = constant, is essentially that shown in Figs. 1 and 2, so the physical ideas and explanations found in the study of the cascade are easily transferred to this three-dimensional case.

Lengths are made dimensionless with respect to the ratio of the speed of sound in the incoming flow to the (constant) angular velocity and velocities with respect to the incoming sound speed. Then lengths are divided by and thus scaled with respect to δ the dimensionless axial chord at the blade hub. Also, δ is chosen as the small parameter; it is numerically small for typical compressor blades. It may be noted that the actual

local chord was not chosen here to scale dimensions because it varies with the span; the axial chord at the hub is the same order as the local chord.

The velocity components relative to the blade in the incoming flow in the x, y, and z directions and the dimensionless radius at which this velocity is sonic are, respectively

$$u_o = [1 + 2\delta r_{so} z + \delta^2 z^2]^{1/2} \tag{16a}$$

$$v_o = 0 \qquad w_o = 0 \tag{16b,c}$$

$$r_{so} = \sqrt{1-M_{oa}^2}$$

where M_{oa} is the Mach number of the (absolute) incoming flow in the axial direction; i.e., it is the Mach number of the flow entering the stage. Thus δ orders the change in velocity which occurs across the blade span as a result of the spanwise variation of the tangential velocity ($r\omega$). On the other hand, the thickness and camber of the blades is $O(\varepsilon^2)$ and so in a channel region between adjacent blades the perturbations in u is $O(\varepsilon)$. It is the order of the ratio δ/ε which characterizes the various problems which may be studied. Because the blades cause the largest changes in the incoming flow when $\delta/\varepsilon = O(1)$, it is this case which is considered here; in particular

$$\varepsilon m = \delta r_{so} \tag{17}$$

where m is an arbitrary constant of O(1).

An analysis of the three-dimensional flow field shows that the various regions found are the same as those which occur in the study of the cascade, illustrated in Fig. 2. The channel flow region is again one-dimensional to

lowest order, but now variations in both y and z are found in higher order terms. In the outer region, a very interesting result is found in that to the lowest order of approximation the flow is two-dimensional with a Mach number equal to the average value over the span of the blade. Again, the outer solutions do not match with the channel flow solutions and so a thin ($O(\epsilon^{1/2})$) inner region is again necessary, and it is the solution in this inner region which has been very difficult to obtain.

In the inner region, the flow changes from a two-dimensional outer flow, in lowest order, to a three-dimensional channel flow. If the velocity is written in terms of a perturbation (from u_0) potential, this perturbation potential can be divided into two parts. Thus, if $\phi_1^*(x^*,y^*,z^*)$ is the lowest order approximation to the perturbation potential and x^*, y^* and z^* are independent variables all in the inner region, one can write

$$\phi_1^* = \phi^{(2)}(x^*,y^*) + \phi_1(x^*,y^*,z^*) \tag{18}$$

where $\phi^{(2)}(x^*,y^*)$ is the known inner solution for a two-dimensional cascade flow written in terms of the parameters of the three-dimensional flow problem. It can be shown that $\phi^{(2)}$ satisfies the matching conditions from the outer flow, the boundary conditions at the surfaces of the blades, and the matching conditions from the solutions in the channel region. It does not satisfy the governing equations and, of course, it does not give any values for w so there is no agreement with channel flow solutions for w. Hence, an additional potential ϕ_1 is needed, satisfying the equation (C_0 is a constant)

$$\frac{z^*}{z^*_{av}}\phi_{1x^*x^*} - \phi_{1y^*y^*} - \frac{1}{C_0}\phi_{1z^*z^*} = -\left(\frac{z^*}{z^*_{av}} - 1\right)\phi^{(2)}_{x^*x^*} \tag{19}$$

where z^*_{av} is the average value of z^* over the span of the blade. The flow

picture seen at any constant radius (z^*), to the scale of the inner region, is shown in Fig. 4. The boundary conditions are simply that at all solid surfaces, the normal derivative of ϕ_1 is zero and as infinity is approached whenever there are no solid surfaces, all derivatives tend to zero. The problem is thus posed as a Neumann problem.

It is necessary to find the solution to Eqn. (19) numerically. Because boundary conditions at infinity are involved, it was decided to transform the physical region into a bounded computational region. This was done in two steps. The first consisted of transforming the flow in the physical plane seen at any radius, as in Fig. 4, to one in an upper half plane at the same value of z. The transformation is, in complex form with $\zeta = \xi + i\eta$,

$$x^* + iy^* = \zeta - 1 - \ln \zeta \tag{20}$$

Next, the field was reduced to one of finite extent by the transformation

$$s = \frac{1}{1+\rho} \tag{21a}$$

$$\rho = \sqrt{\xi^2+\eta^2} \qquad \theta = \tan^{-1}\left(\frac{\eta}{\xi}\right) \tag{21b,c}$$

where ρ and θ are polar coordinates in the intermediate plane defined by Eqn. (20). The net result is a three-dimensional rectangular computational domain defined by $0 \leq s \leq 1$, $0 \leq \theta \leq \pi$, and $z_h \leq z \leq z_t$. The subscripts t and h refer to conditions at the blade tip and the hub, respectively. Physically, the boundary plane at s = 0 corresponds to the flow field at $\rho = \infty$, far from the channel, and the boundary plane at s = 1 corresponds to the flow in the channel as $x^* \to \infty$. The transformed equation for ϕ_1 is relatively long and complex and will not be given here.

Although the problem of boundary conditions at infinity is taken care of by the transformation, it is easily shown that if $\phi_1(x^*,y^*,z^*) = \phi(s,\theta,z^*)$, then

$$\phi_{1x^*} \sim (1-s)\phi_s + \ldots \tag{22}$$

Hence, since the boundary condition $\phi_{1x^*} \to 0$ as $x^* \to \infty$ corresponds to a condition on ϕ_s as $s \to 1$, it is seen from Eqn. (22) that the corresponding condition on ϕ_s cannot be found. Several methods by which this difficulty could be remedied were tried. For example, if the velocity ϕ_{1x^*} rather than the potential ϕ_1 were to be sought, then the problem is a Dirichlet rather than a Neumann problem and the difficulty with the boundary condition is removed; the governing equation is also easily modified so as to be written in terms of ϕ_{1x^*}. However, one must then deal with the singularity in the velocity at the leading edge of the blade typically found in inviscid airfoil theory. Two-dimensional model problems were considered with the same kind of singularity and it was found that there was apparently no way to handle this type of singularity adequately using the finite difference schemes one is forced to use, due to financial constraints, when three-dimensional flows are considered.

After discussion of this problem with several experts in numerical methods over the country, it was decided to solve a mixed problem for ϕ_1 in which the normal derivatives at solid surfaces are set equal to zero, an arbitrary value for ϕ_1 is set at $s = 0$, and the unknown constant ϕ_1 at the $s = 1$ plane is found by using the numerical boundary condition $\phi_{ss} = 0$ there. This procedure worked very well in the model problems and can be shown to restrict computational errors to a thin region near $s = 1$, in which,

because of matching conditions, the solution is known. Although some difficulties in rates of convergence still exist, it is believed that these problems are now solvable and solutions are being obtained. It should be noted that because 30 mesh points in the s and z directions and 10 to 20 in the θ direction are being used, a relatively large amount of memory is required for the SOR techniques being employed. Programs to transform the solutions back to the physical plane in terms of velocities have been completed as have those for lines of constant velocity.

It remains to program the known upstream solutions and then form composite solutions valid everywhere in the field. This is being done. Results will be shown in the form of pressure distribution on the blades, and lines of constant velocity or Mach number.

(3) Supersonic Turbulent Boundary Layer at a Ramp

When a turbulent boundary layer at supersonic speed encounters a shallow compression corner, details of the local mean flow are determined by an interaction between the boundary layer and an oblique shock wave. For an unseparated flow, the shock wave forms at a distance from the corner which is quite small in comparison with the boundary-layer thickness, and the initial rise in pressure is very steep. The subsequent more gradual pressure increase continues for a distance of perhaps a few boundary-layer thicknesses, depending on the local Mach number (e.g., Ref. 2).

In these regions near the corner, the mean fluid acceleration has much larger magnitude than in the undisturbed boundary layer, and the pressure gradient is much larger than the perturbation in the force due to Reynolds

shear stresses. Changes in the mean flow properties may then be described approximately by inviscid-flow equations, except at points in a thinner sublayer, very close to the surface. That is, if suitable asymptotic expansions for small nondimensional friction velocity, and therefore large Reynolds number, are substituted into the averaged Navier-Stokes equations, it is found that the largest terms satisfy inviscid-flow equations. This formulation has been used previously in studies of the closely related flow problem of interaction at transonic speeds between an unseparated turbulent boundary layer and a normal shock wave (e.g., Refs. 3-7). Other turbulent boundary-layer interactions which have been studied in this way include the subsonic flow at a trailing edge (e.g., Ref. 7) and the incompressible flow over a shallow bump.[8]

The present investigation was motivated largely by the work of Roshko and Thomke,[2] which included measurements of surface pressure for a wide range of Mach numbers and corner angles. They also demonstrated that numerical calculations by the method of characteristics agree very closely with experimental data for most of the gradual part of the pressure rise. This agreement provides strong support for the use of an inviscid-flow approximation. However, their calculation introduced a supersonic slip velocity at the wall, and an estimate of the "slip Mach number" was required.[2],[9]

The purposes of the present work have been to obtain analytical solutions for the portion of the pressure rise calculated numerically in Refs. 2 and 9, to explore in a systematic way the implications of an asymptotic inviscid-flow description at smaller distances from the corner, and to

attempt a prediction of the surface shear-stress distribution, all for unseparated flow.

A sketch of the mean flow field is shown in Fig. 5. The mean velocity profile in the undisturbed boundary layer is described by the velocity-defect law and the law of the wall, suitably modified for compressible flow.[10],[11] The corner angle is $\varepsilon << 1$ and the nondimensional friction velocity is $u_\tau << 1$, where the reference velocity is the undisturbed external-flow velocity. Solutions have been obtained using the method of matched asymptotic expansions, in the limit as $\varepsilon \to 0$ and $u_\tau \to 0$ such that also $u_\tau/\varepsilon \to 0$. Outer solutions, for a transverse length scale equal to the boundary-layer thickness, have been derived in supersonic, hypersonic, and transonic small-disturbance limits. A number of different intermediate solutions have been found for smaller distances from the corner. Finally, the solution in an appropriate sublayer limit allows calculation of the wall shear-stress distribution downstream of the corner. These solutions are described in somewhat greater detail in the following paragraphs.

In the supersonic small-disturbance limit, with the boundary-layer thickness as the length scale, the shock wave and the outgoing characeristics have the same slope. The surface pressure changes continuously because of incoming disturbances which result from the continuous reflection of the shock wave as it passes through the boundary layer. The solution for pressure has a constant part equal to the value for uniform flow past a corner and a variable part derived from a perturbation velocity potential which satisfies a wave equation. The boundary condition at the shock wave is obtained from the shock-polar equation, and also requires

calculation of the small change in vorticity across the shock. A tangency condition is imposed at the surface, since it can be shown that the displacement effect due to deceleration of fluid close to the surface is of higher order.

For higher values of the Mach number M_∞ the flow is studied in a hypersonic small-disturbance limit. The shock wave now is no longer weak, and is inclined at a shallow angle $O(\varepsilon)$. Disturbances in the flow behind the shock wave will overtake and be reflected from the shock, giving additional contributions to the surface pressure. The vorticity, however, is small enough that reflections of small disturbances within the boundary-layer region between the shock and the wall are found to be of higher order. As in the supersonic limit, the constant part of the pressure is the same as for uniform flow past a corner and the variable part is determined by solving a wave equation subject to the flow tangency condition at the surface and the shock-wave jump conditions. Now, however, these boundary conditions lead to a functional equation, in the same form as obtained by others for uniform flow past a wedge-like shape with small perturbations in surface slope.[12],[13] The functional equation has a solution in the form of an infinite series.

Neither the supersonic or the hypersonic solution alone gives good agreement with the data of Roshko and Thomke. A composite supersonic-hypersonic solution leads to improved but still not satisfactory agreement, with an error which grows as the distance from the corner decreases. The inaccuracy arises because these solutions use the external-flow velocity as a first approximation to the mean velocity within the boundary

layer, and is related to the logarithmic behavior of the undisturbed velocity profile. By a careful study of intermediate limits of the equations, in a manner first suggested for another flow problem in Ref. 6, still better agreement with experiment can be achieved. The supersonic-hypersonic solution is thereby modified, with the help of "supersonic intermediate solutions," so as to remain uniformly valid over an extended range which includes points much closer to the corner.

This combined solution leads to the following expression for the predicted surface pressure:

$$p = p_1 + \frac{\varepsilon\gamma}{B_0} + \frac{\varepsilon^2\gamma}{4}\left[\frac{M_0^2\{(M_0^2-2)^2 + \gamma M_0^4\}}{B_0^4} - (\gamma+1)B_0^2\right]$$

$$- \gamma p_1 \tilde{B}_0 M_0^2 \frac{A_0 U_0'}{B_0^2 U_0}\sigma + u_\tau \gamma p_1 \frac{\tilde{B}_0 M_0^2 A_0 U_0'}{B_0^2 U_0}\tilde{f}(\tilde{x}) + \ldots, \qquad (24)$$

Here p has been made nondimensional with the undisturbed pressure, γ is the ratio of specific heats, x is a coordinate made nondimensional with the boundary-layer thickness and measured along the surface downstream from the corner, and

$$U_0 = \Gamma \sin\{\sin^{-1}\frac{1}{\Gamma} + (\frac{\gamma-1}{2}M_\infty^2)^{1/2}\sigma\} \qquad (25a)$$

$$U_0' = \{1 + \frac{\gamma-1}{2}M_\infty^2(1 - U_0^2)\}^{1/2} \qquad (25b)$$

$$M_0 = \frac{M_\infty U_0}{U_0'} \qquad (25c)$$

$$B_0^2 = M_0^2 - 1 \qquad (25d)$$

$$\sigma = \frac{u_\tau}{\kappa} \ln \frac{x}{B_0} \qquad \kappa \approx 0.41 \tag{25e,f}$$

$$\Gamma = \left\{\frac{2 + (\gamma-1)M_\infty^2}{(\gamma-1)M_\infty^2}\right\}^{1/2} \tag{25g}$$

$$A_0 = (M_0^2-2)\left(1 - \frac{\gamma-1}{2} M_0^2\right)/B_0^2 \tag{25h}$$

$$P_1 = 1 + \gamma B_0^2 \varepsilon^2 s_1 \tag{25i}$$

$$s_1 = \frac{\gamma+1}{4} + \left\{\left(\frac{\gamma+1}{4}\right)^2 + \frac{1}{B_0^2\varepsilon^2}\right\}^{1/2} \tag{25j}$$

$$\tilde{B}_0 = B_0\varepsilon \left(\frac{s_1}{s_1-1} \frac{1}{P_1}\right)^{1/2} \tag{25k}$$

$$\tilde{x} = \varepsilon x \tag{25l}$$

$$\tilde{f} = u_{01}\left(\frac{s_1 x}{1+\tilde{B}s_1-\tilde{B}}\right) + \ldots \tag{25m}$$

The velocity defect in the outer part of the undisturbed boundary layer is $u_\tau u_{01}(y)$, where y is a coordinate made nondimensional with the boundary-layer thickness and measured normal to the surface. The single term shown for the function $\tilde{f}$ is the first term of the infinite-series solution to the functional equation mentioned earlier.

Calculation of the pressure according to this formula does not require the introduction of a "slip Mach number" as in the calculation of Ref. 2. Rather, the solution simply requires substitution of values for x and for the parameters. In Fig. 6 it is shown that this modified solution for the

surface pressure gives excellent agreement with experiment for $M_\infty \approx 5$ and $\varepsilon \approx 15°$. The Reynolds number based on boundary-layer thickness in this case is about 5×10^6. Similar agreement is found for $M \approx 4$ and $\varepsilon \approx 15°$. Agreement with a numerical solution obtained by Roshko and Thomke using the method of characteristics is equally good. In a comparison at $M_\infty \approx 3$ and $\varepsilon \approx 10°$, however, the theoretical prediction lies about 8% below the experimental values over a similar range of distance.

At a still lower Mach number, $M_\infty \approx 2$, for $\varepsilon \approx 5°$, the data show a completely different trend. A rather high maximum pressure is reached slightly downstream of the corner, and the pressure then decreases toward the final value. For parts of the boundary layer where the Mach number M has low supersonic values, the incoming waves, due to reflection of the shock wave, are expansions rather than compressions; in the linear approximation the change occurs when $M \approx \sqrt{2}$. Roshko and Thomke suggested that the reversal of the pressure gradient at the surface may be associated with the sign change of the reflected waves. However, the present solutions show that this effect occurs over a far smaller length scale than is shown by the experiments. This conclusion is based on detailed derivations of "transonic intermediate solutions" corresponding to points in the boundary layer where M is close to 1. An inviscid-flow description therefore does not seem capable of reproducing the measured pressure distribution for this case. It does seem possible, however, that the presence of a shallow separation bubble, perhaps of length comparable with the boundary-layer thickness, might lead to a pressure distribution of the form observed.

At the higher Mach numbers where good agreement between theory and experiment is obtained, it is anticipated that an extremely short separation bubble is present. Measurements by a "liquid-line" technique (e.g., Ref. 14) have been able to detect bubbles as short as perhaps one-tenth of a boundary-layer thickness for values of the parameters similar to those quoted above. Roshko and Thomke[15] gave an empirical formula for an interaction length, and proposed two different values of this length as corresponding to inciplient separation detected by surface-flow or pressure measurements. An extrapolation of this idea for one of the cases considered above would imply a separation bubble with length of about one per cent of a boundary-layer thickness. This length, however, is comparable with the length scales for intermediate solutions corresponding to distances from the corner such that the local Mach number is close to one. These "transonic intermediate solutions" therefore seem useful for predicting the pressure at best for very small corner angles. Moreover, it seems possible that oscillations of the shock wave due to turbulent fluctuations might tend to smear out the measured pressure distributions for these very small distances. The transonic intermediate solutions do serve the purpose of showing that the measured pressures for $M_\infty \approx 2$ can not be predicted using inviscid-flow equations. The supersonic intermediate solutions, on the other hand, are essential for the accuracy shown in Fig. 6. A comparison for points very close to the corner is not shown in Fig. 6, since, as noted above, the theory appears inapplicable there, and since experimental results are not available for distances from the corner smaller than a few per cent of the boundary-layer thickness.

The largest terms in the "outer" solutions given earlier are derived from inviscid-flow equations, and therefore can not be expected to contain enough information for calculation of changes in the wall shear stress. Instead, the flow details must also be studied in a sublayer where the changes in turbulent stresses are important. This sublayer will play the role of a new, thinner boundary layer, in an inviscid rotational external flow described by the outer solutions. From a different view, the Reynolds stress in the very thin wall layer will be nearly in equilibrium with the local value of the wall shear stress, and can not be expected to match with the Reynolds stress in the outer part of the boundary layer, which depends primarily on upstream history. Instead, the perturbations in the wall-layer solution and in the outer solution are to be matched with the perturbations in the sublayer. This sublayer has been called a "Reynolds-stress sublayer"[5],[6] or a "blending layer."[3],[7]

Terms of order ε and ε^2 in the non-dimensional shear stress do not depend on solution of a sublayer equation, but terms of order εu_τ are found by solving a momentum equation of boundary-layer type, which expresses a balance of Reynolds-stress, pressure and inertia terms in a sublayer having thickness smaller than the boundary-layer thickness by a factor u_τ. An approximate solution has been obtained using a Prandtl mixing-length representation. The result for one case is compared with experiment[16] in Fig. 7. Except for points very close to the corner, the form of the shear stress is predicted accurately, but the theoretical values are everywhere roughly 10% too high.

In summary, the composite of supersonic and hypersonic, outer and intermediate solutions for surface pressure gives excellent agreement with experiment for $M_\infty \approx 4$ or $M_\infty \approx 5$ and $\varepsilon \approx 15°$; transonic intermediate solutions suggest that the same type of asymptotic formulation is not adequate for $M_\infty \approx 2$ and $\varepsilon \approx 5°$, and experiments also indicate that a very short separation bubble influences the flow close to the corner at the higher Mach numbers; and approximate solution of a sublayer momentum equation gives fair agreement with measured wall shear stresses in a particular case.

A Ph.D. dissertation covering this work has been completed. A paper is in preparation for journal publication.

BIBLIOGRAPHY

1. Messiter, A. F. and Adamson, T. C., Jr. (1981). "Transonic small-disturbance theory for lightly loaded cascades," AIAA Journal, vol. 19, no. 8, pp. 1047-1054.

2. Roshko, A. and Thomke, G. J. (1969). "Supersonic turbulent boundary-layer interaction with a compression corner at very high Reynolds number." Proc. ARL Symp. on Viscous Interaction Phenomena in Supersonic and Hypersonic Flow. Univ. of Dayton Press, Dayton, Ohio, pp. 109-138.

3. Melnik, R. E. and Grossman, B. (1974). "Analysis of the ineraction of a weak normal shock wave with a turbulent boundary layer." AIAA Paper No. 74-598, AIAA 7th Fluid and Plasma Dynamics Conference, Palo Alto, California.

4. Messiter, A. F. (1980). "Interaction between a normal shock wave and a turbulent boundary layer at high transonic speeds. Part I: Pressure distribution." ZAMP, vol. 31, pp. 204-226.

5. Adamson, T. C.,Jr., and Liou, M. S. (1980). "Interaction between a normal shock wave and a turbulent boundary layer at high transonic speeds. Part II: Wall shear stress." ZAMP, vol. 31, pp. 227-246.

6. Adamson, T. C., Jr., Liou, M. S. and Messiter, A. F. (1980). "Interaction between a normal shock wave and a turbulent boundary layer at high transonic speeds." NASA CR 3194.

7. Melnik, R. E. (1981). "Turbulent interactions on airfoils at transonic speeds — recent developments." Paper No. 10, AGARD-CP-291.

8. Sykes, R. I. (1980). "An asymptotic theory of incompressible turbulent boundary-layer flow over a small hump." Journal of Fluid Mechanics, vol. 101, pt. 3, pp. 647-670.

9. Rosen, R., Roshko, A. and Pavish, D. L. (1980). "A two-layer calculation for the initial interaction region of an unseparated supersonic turbulent boundary layer with a ramp." AIAA Paper 80-0135, AIAA 18th Aerospace Sciences Meeting, Pasadena, California.

10. Van Driest, E. R. (1951). "Turbulent boundary layer in compressible fluids." Journal of Aeronautical Sciences, vol. 18, pp. 145-160.

11. Maise, G. and McDonald, H. (1968). "Mixing length and kinematic eddy viscosity in a compressible boundary layer." AIAA Journal, vol. 6, no. 1, pp. 73-80.

12. Chu, B. T. (1952). "On weak interaction of strong shock and Mach waves generated downstream of the shock." J. Aero. Sci., vol. 19, no. 7, pp. 433-446.

13. Guiraud, J. P. (1957). "Écoulements hypersoniques infiniment voisins de l'écoulement sur un dièdre." Comptes Rendus Acad. Sci. Paris, vol. 244, no. 18, pp. 2281-2284.

14. Appels, C. and Richards, B. E. (1975). "Incipient separation of a compressible turbulent boundary layer." Paper No. 21, AGARD-CP-168.

15. Roshko, A. and Thomke, G. J. (1976). "Flare-induced separation lengths in supersonic turbulent boundary layers." AIAA Journal, vol. 14, no. 7, pp. 873-879.

16. Settles, G. S., Fitzpatrick, T. J. and Bogdonoff, S. M. (1979). "Detailed study of attached and separated compression corner flowfields in high Reynolds number supersonic flow." AIAA Journal, vol. 17, no. 6, pp. 579-585.

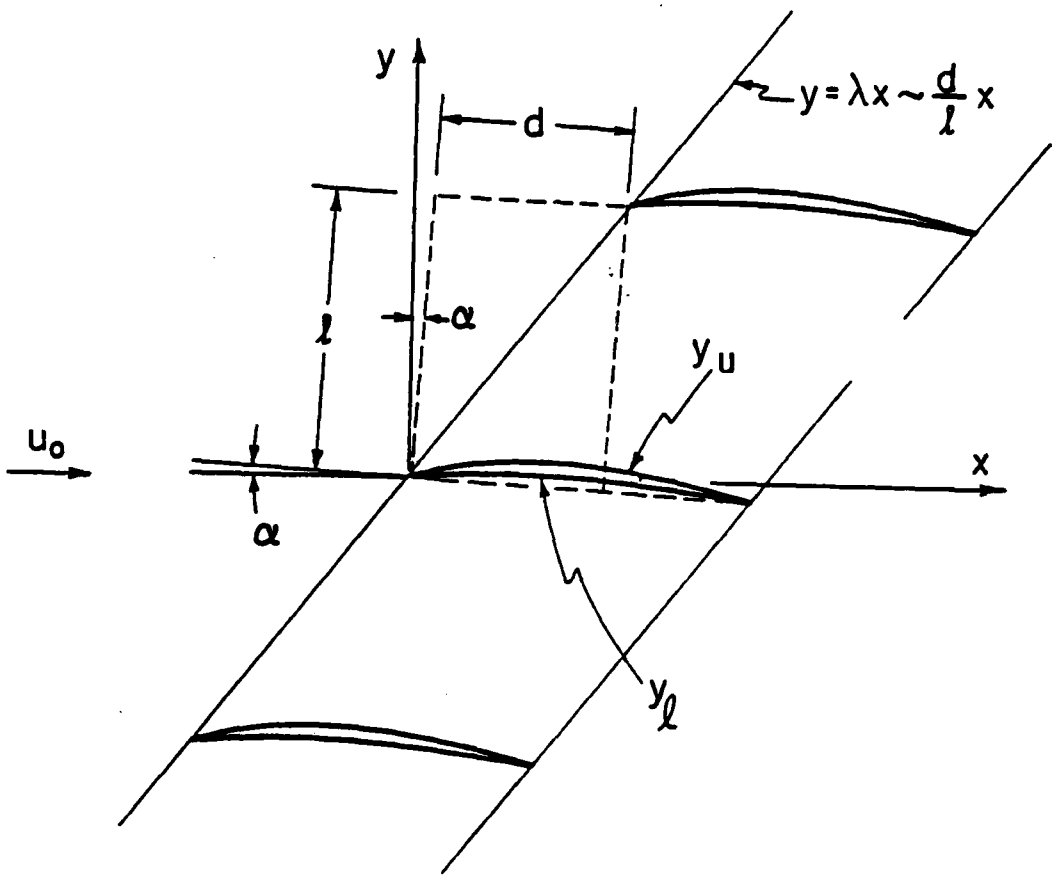

Figure 1. Flow geometry

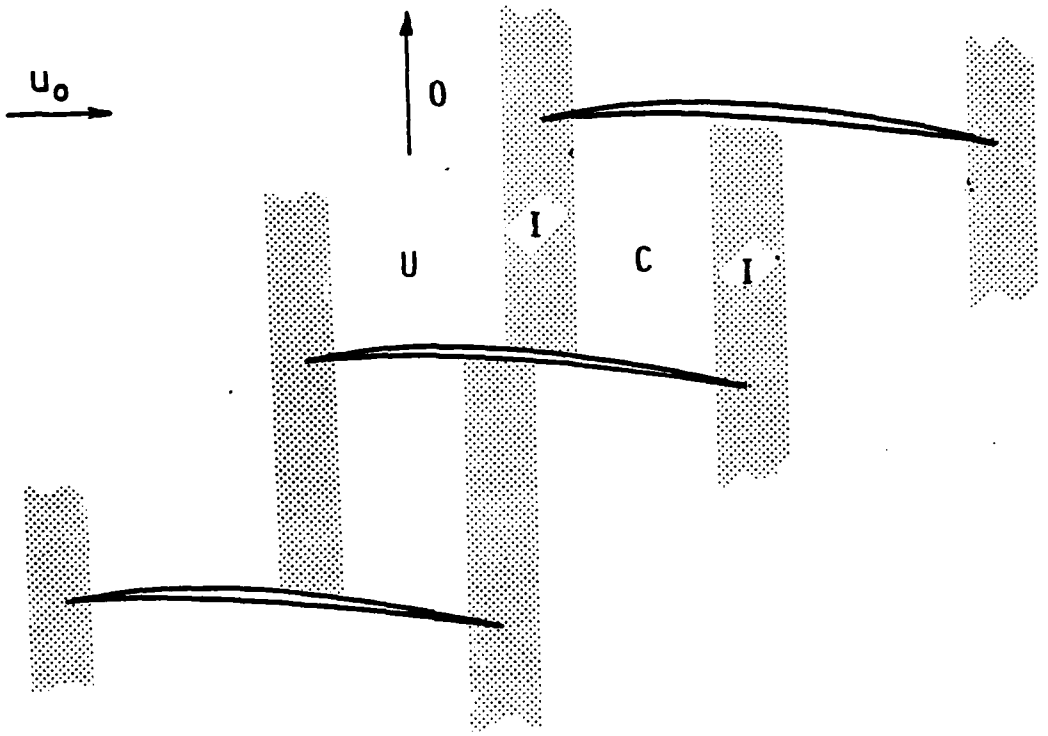

Figure 2. Asymptotic flow description.

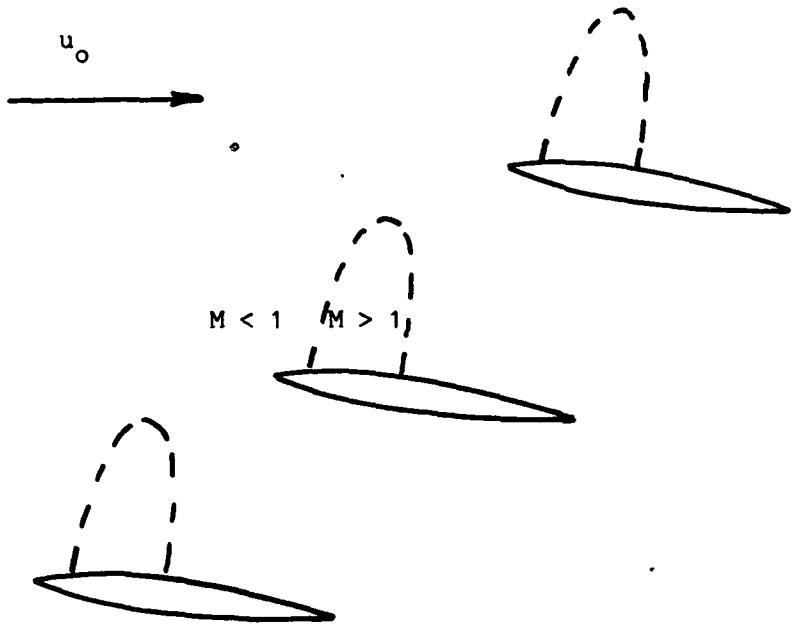

Figure 3. Heavily loaded cascade with supercritical flow; shockless flow case shown.

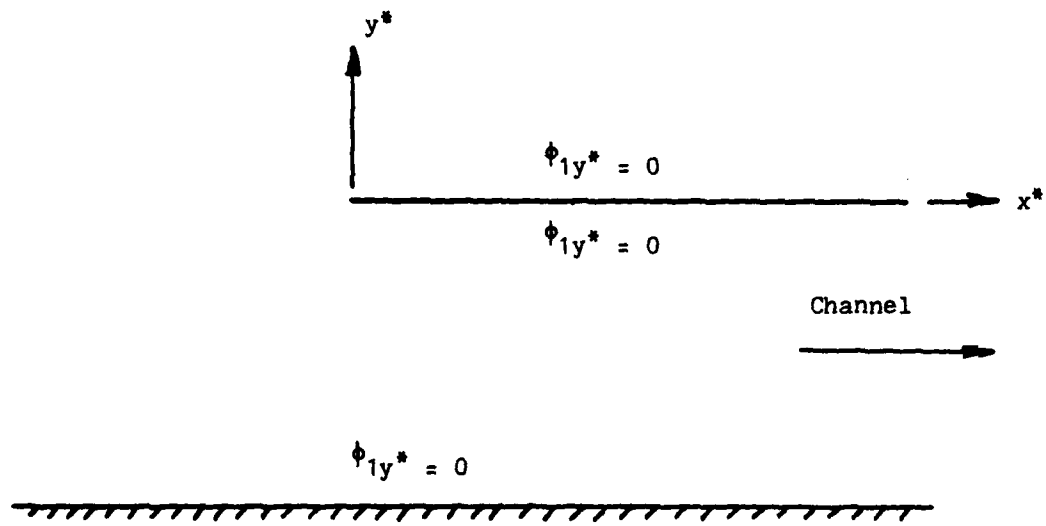

Figure 4. Coordinate system and boundary conditions in inner region.

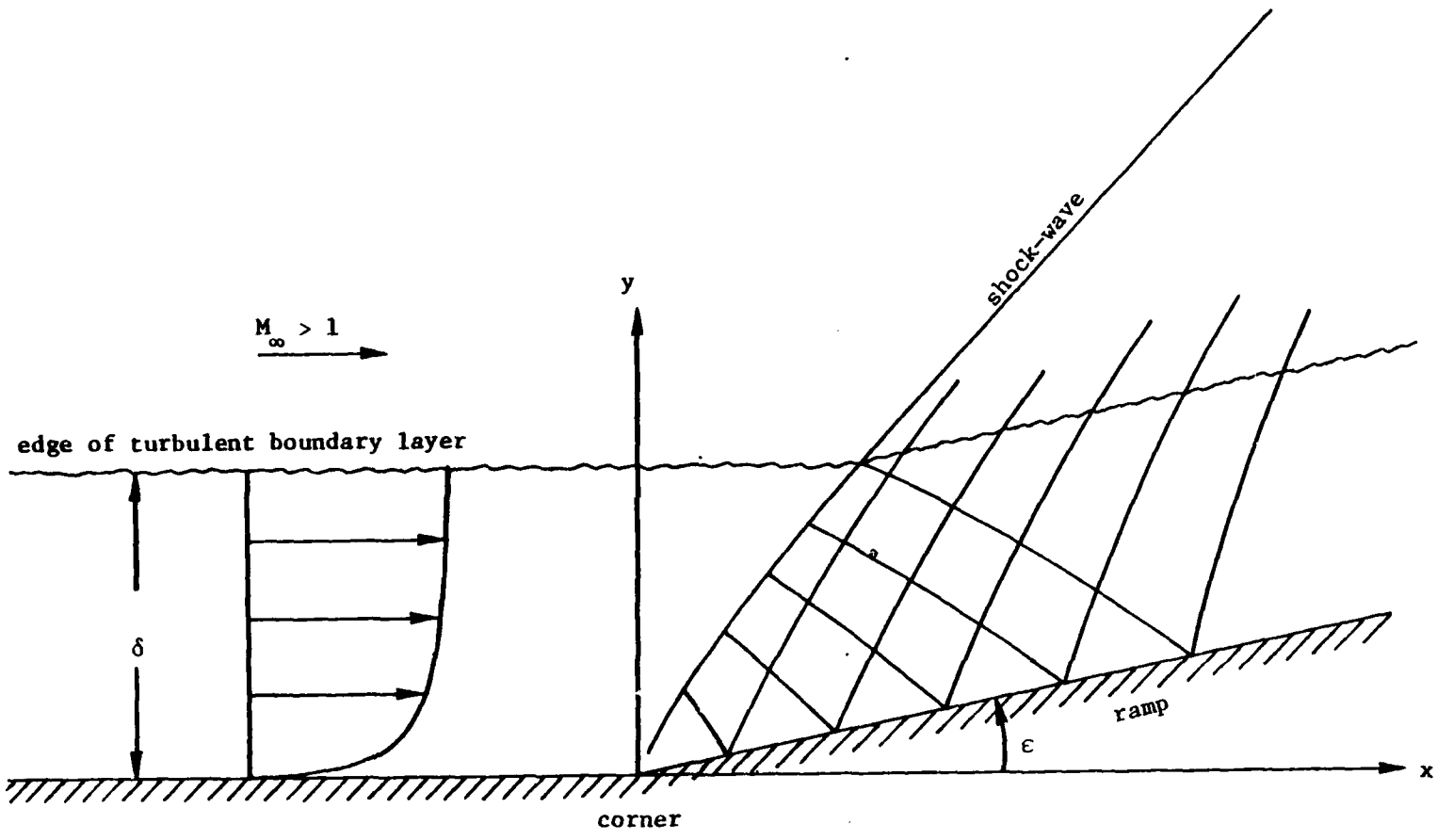

Figure 5. Sketch showing the turbulent boundary layer, the shock wave, and the ramp.

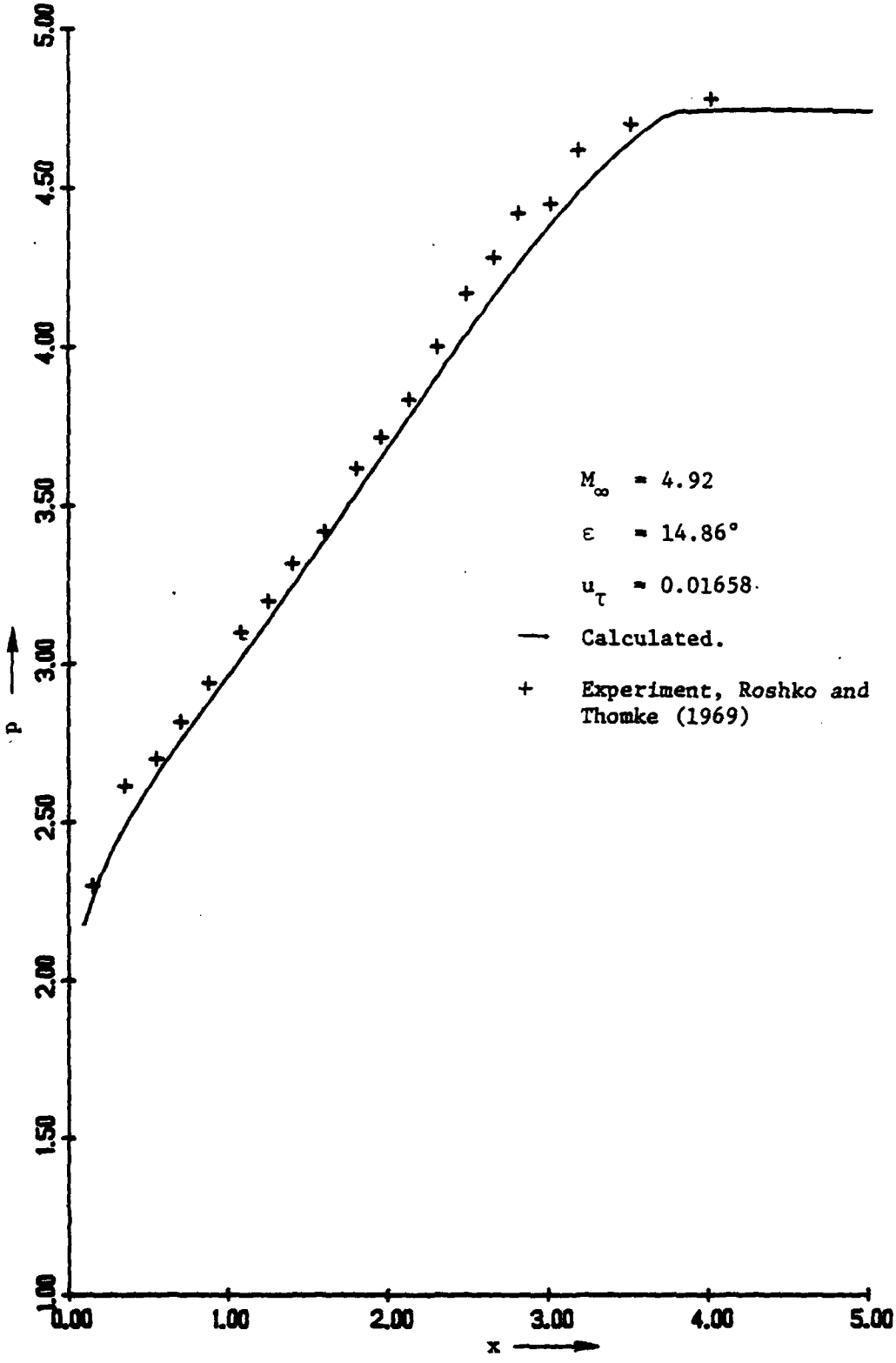

Figure 6. Wall pressure using the composite supersonic-hypersonic solution.

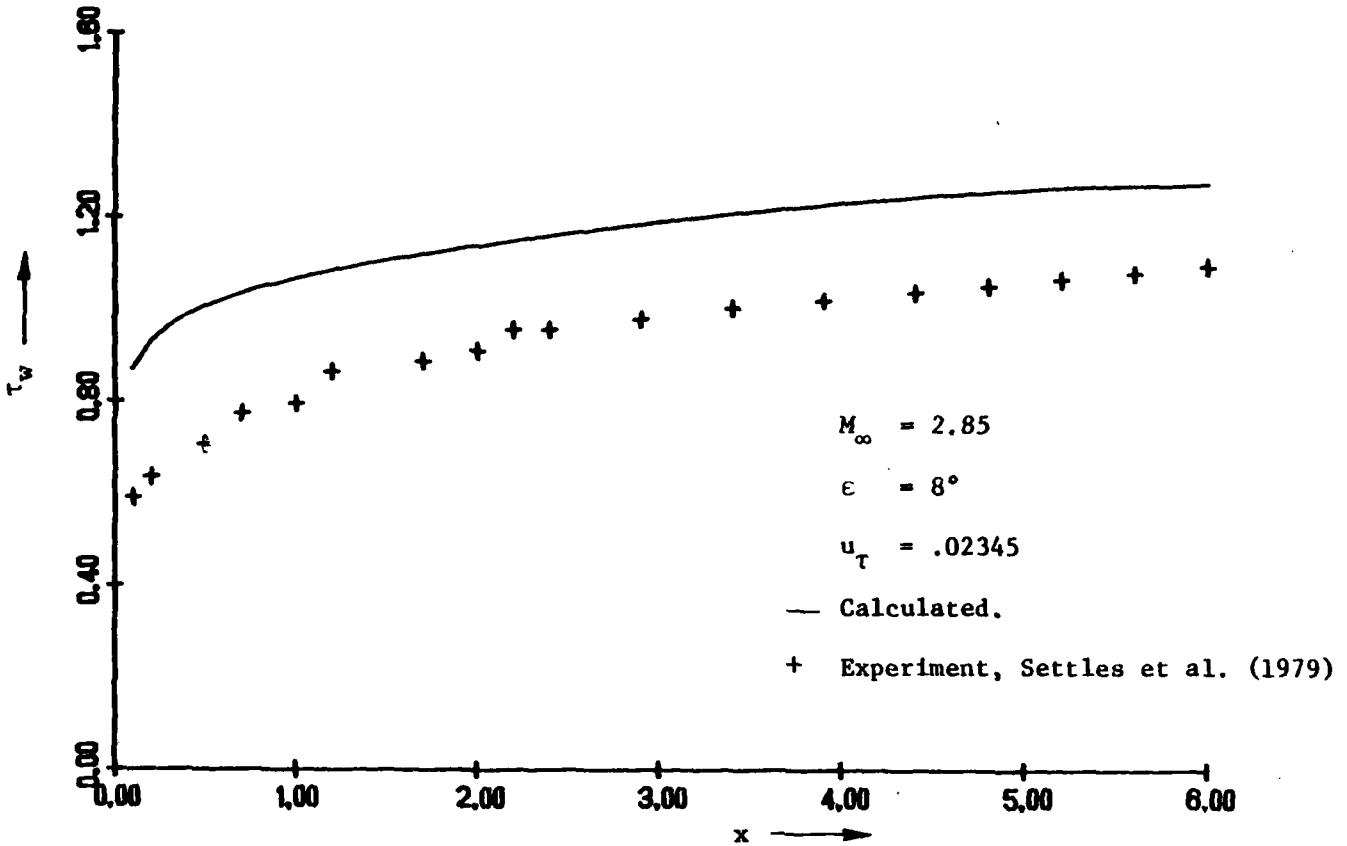

Figure 7. Wall shear stress using the composite solution.

DISTRIBUTION LIST
INTERNAL FLOW AND COMBUSTION

One copy except as noted

Mr. M. Keith Ellingsworth
Mechanics Division
Office of Naval Research
800 N. Quincy Street
Arlington, VA 22217

Defense Documentation Center — 12
Building 5, Cameron Station
Alexandria, VA 22314

Technical Information Division — 6
Naval Research Laboratory
4555 Overlook Avenue, S.W.
Washington, DC 20375

Dr. Gerhard F. Heiche
Code 03D
Naval Air Systems Command
Washington, DC 20361

Dr. E. S. Oran
Code 6020
Naval Research Laboratory
4555 Overlook Avenue, S.W.
Washington, DC 20375

Library
Naval Postgraduate School
Monterey, CA 93940

Director
Turbopropulsion Laboratory
Naval Postgraduate School
Monterey, CA 93940

Chairman
Department of Aeronautics
Naval Postgraduate School
Monterey, CA 93940

Chairman
Department of Mechanical Engineering
Naval Postgraduate School
Monterey, CA 93940

Dr. Julian Tishkoff
AFOSR/NA, Bldg. 410
Bolling AFB
Washington, DC 20332

Professor J. L. Lumley
123 Day Hall
Cornell University
Ithaca, NY 14853

Professor C. T. Bowman
Dept. of Mechanical Engineering
Stanford University
Stanford, CA 94043

Prof Thomas C. Adamson, Jr.
Dept. of Aerospace Engineering
University of Michigan
Ann Arbor, MI 48109

Professor J. P. Johnston
Dept. of Mechanical Engineering
Stanford University
Stanford, CA 94305

Professor Paul A. Libby
Applied Mechanics & Engineering
Sciences
University of California
La Jolla, CA 92093

Professor Anatol Roshko
Div. of Engineering & Applied Science
California Institute of Technology
Pasadena, CA 91125

Prof. R. K. Chang
Dept. of Engineering & Applied
Science
Yale University
New Haven, CT 06520

Prof. E. Hirleman
Mechanical Engineering Dept.
Arizona State University
Tempe, AZ 85821

Prof. C. Wittig
Dept. of Electrical Engineering
University of Southern California
University Park
Los Angeles, CA 90007

Professor E. Covert
Dept. of Aeronautics and Astronautics
Massachusetts Institute of
Technology
Cambridge, MA 02139

Professor F. A. Sisto
Dept. of Mechanical Engineering
Stevens Institute of Technology
Castle Point Station
Hoboken, NJ 07030

Professor R. L. Simpson
Civil & Mechanical Engineering
Southern Methodist University
Dallas, TX 75275

Professor Warren C. Strahle
School of Aerospace Engineering
Georgia Institute of Technology
Atlanta, GA 30332

Professor C. K. Law
Mechanical & Nuclear Engineering
Department
Northwestern University
Evanston, IL 60201

Dr. R. M. Moriarty
Department of Chemistry
University of Illinois -Chicago
Chicago, IL 60680

Dr. M. Sajben
McDonnell Douglas Research Lab.
Box 516
St. Louis, MO 63166

Dr. G. Dobbs
United Technologies Research
Center
East Hartford, CT 06108

Dr. Marshall Lapp
General Electric Research
Development Center
P.O. Box 43
Schenectady, NY 12301